J Therm Anal Calorim (2014) 116:77–91
DOI 10.1007/s10973-014-3702-x

Synthesis, thermal, spectral and biological properties of zinc(II) 4-hydroxybenzoate complexes

Katarína Homzová · Katarína Győryová · Zuzana Bujdošová · Daniela Hudecová · Mária Ganajová · Zuzana Vargová · Jana Kovářová

Received: 8 July 2013 / Accepted: 16 February 2014 / Published online: 21 March 2014

Abstract New zinc(II) 4-hydroxybenzoate complex compounds with general formula $[Zn(4\text{-}OHbenz)_2L_n]\cdot xH_2O$, where 4-OHbenz = 4-hydroxybenzoate; L = isonicotinamide, *N*-methylnicotinamide, *N*,*N*-diethylnicotinamide, thiourea, urea, phenazone, theophylline, methyl-3-pyridylcarbamate; $n = 2, 3$; $x = 0–3, 5$, were synthesized and characterised by elemental analysis, thermal analysis and IR spectroscopy. The thermal behaviour of the prepared compounds was studied by TG/DTG and DTA methods in argon atmosphere. The thermal decomposition of hydrated compounds started with dehydration. During the thermal decomposition, organic ligand, carbon monoxide, carbon dioxide and phenol were evolved. The final solid product of the thermal decomposition was zinc or zinc oxide. The volatile gaseous product, solid intermediate products and the final product of thermal decomposition were identified by IR spectroscopy, mass spectrometry, qualitative chemical analyses and X-ray powder diffraction method. The antimicrobial activity of zinc(II) carboxylate compounds was tested against various strains of bacteria, yeasts and filamentous fungi (*S. aureus, E. coli, C. parapsilosis, R. oryzae, A. alternata, M. gypseum*). The presence of zinc in complexes led to the increase in their antimicrobial activity in comparison with free 4-hydroxybenzoic acid.

Keywords Zinc · 4-Hydroxybenzoate · Thermal · Spectral · Biological properties

K. Homzová (✉) · K. Győryová · M. Ganajová · Z. Vargová
Department of Chemistry, Faculty of Science, P. J. Šafárik University, Moyzesova 11, 041 54 Košice, Slovak Republic
e-mail: katarina.homzova@student.upjs.sk; katarina.gyoryova@upjs.sk

Z. Bujdošová
Department of Chemistry, Biochemistry and Biophysics, University of Veterinary Medicine and Pharmacy in Košice, Komenského 73, 041 81 Košice, Slovak Republic

D. Hudecová
Department of Biochemistry and Microbiology, Slovak University of Technology, Radlinského 9, 812 37 Bratislava, Slovak Republic

J. Kovářová
Institute of Macromolecular Chemistry, AS CR, Heyrovsky Sq. 2, 162 06 Prague 6, Prague, Czech Republic

Introduction

Zinc is one of the most important trace elements, which is connected with many biological functions in the body. It forms part of more than 300 metalloenzymes. Zinc is required to maintain normal biochemical function in cells. It is also a structural and catalytic cofactor of metalloproteins, hormones and polynucleotides. Its lack in an organism can cause serious harm and diseases [1].

Zinc(II) carboxylates form a part of coordination compounds that are studied here from the chemical and also biological viewpoints. They are of interest in the field of synthetic and bioinorganic chemistry because of their key role in biological systems. Zinc complexes are used in the treatment of several diseases, for example, Zn(II) acetate with erythromycin is successfully applied in clinical medicine for acne therapy [2]. Benzoate complexes with nicotinamide are used in dermatology as fungicidal treatment for fungal skin diseases [3, 4]. It was found that antiinflammatory and antibacterial activity of metal complexes were higher than the activity of the parent carboxylic acids [5, 6]. On the other hand, some of the aromatic carboxylic acids (like benzoic or cinnamic acid) are known for their antibacterial and antifungal properties. Hydroxybenzoic acids (such as salicylic acid and its derivatives, acetylsalicylic or

5-chlorosalicylic acid) are used in medicine as analgesic, antipyretic and antiinflammatory drugs [7].

It is well documented that the presence of an organic bioactive ligand in the zinc complexes increases their bioactivity [8]. Theophylline is a naturally occurring alkaloid having anti-inflammatory effects in asthma [9], *N*,*N*-diethylnicotinamide is respiration stimulant [10] and phenazone has an analgesic and antipyretic effect [11]. Tarushki et al. [12] synthesized the neutral mononuclear zinc complexes with oxolinic acid. The ability of the studied compounds to bind to calf thymus DNA was proved by UV spectroscopy. From zinc(II), hydroxybenzoates are the most studied 2-hydroxybenzoates (salicylates). It was solved several crystal structures of zinc(II) hydroxybenzoates. In compound, $[Zn(2\text{-}OHbenz)_2{\cdot}2H_2O]$ is zinc in tetraedric surroundings with two water and two carboxylate oxygen atoms [13]. In compound, $[Zn(2\text{-}OHbenz)_2(bipy)(MeOH)]$ is zinc in octaedric surroundings with one monodentate and bidentate chelating coordination of oxygen atom from salicylato ligand, one oxygen atom from methanol and two nitrogen atoms of the chelating 2,2′-bipyridyl [14]. Lemoine et al. [15] prepared and studied crystal structures and anticonvulsant activities of ternary $[Zn(3,5\text{-diisopropyl-}2\text{-}OHbenz)_2]$ and $[Zn(2\text{-}OHbenz)_2]$ complexes. Sokolík et al. [16] studied antiinflammatory activities of compounds with the formula $[M(H_2O)_2(3,6\text{-dimethyl-}2\text{-}OHbenz)_2]{\cdot}2H_2O$, where M = Zn(II), Cu(II). Olczak-Kobza et al. [17, 18] prepared and characterised zinc(II) and cadmium(II) salicylates of the type $[M(2\text{-}OHbenz)_2L_2]$, where L = imidazole, 2-methylimidazole, 4-methylimidazole by thermal and X-ray methods. Chomič et al. [19] studied thermal properties of zinc(II) salicylate complex compounds of the type $Zn(2\text{-}OHbenz)_2L_2{\cdot}nH_2O$, (L = thiourea, nicotinamide, caffeine and theobromine; n = 2–4). Bujdošová et al. [20–22] prepared zinc(II) 4-chloro- and 5-chloro-salicylates of the type $[Zn(Cl\text{-}2\text{-}OHbenz)_2(L)_n(H_2O)_x]$, (L = *N*,*N*-diethylnicotinamide, isonicotinamide, theophylline, methyl-3-pyridylcarbamate, phenazone; n = 1, 2; x = 0, 1, 2, 4) and studied their thermal, spectral and biological properties. Köse et al. [23, 24] prepared 3-hydroxybenzoate complexes $[M(3\text{-}OHbenz)_2(nad)_2(H_2O)_2]$, where M = Zn(II), Co(II), Ni(II) and Cu(II) and studied their spectral, thermal and magnetic properties. Zaman et al. [25] studied crystal structure of $[Zn(inad)_2(H_2O)_4](3\text{-}OHbenz)_2{\cdot}4H_2O$, where zinc is coordinated with four oxygen atoms from water in the equatorial plane and octahedral geometry is completed with two nitrogen atoms from two isonicotinamide ligands. Icbudak et al. [26] synthesized and characterised $[Zn(4\text{-}OHbenz)_2(nad)_2]$ and compounds with the formula $[M(4\text{-}OHbenz)_2(dnad)_2(H_2O)_2]{\cdot}2H_2O$, where M = Zn(II), Ni(II). There was studied physicochemical properties but in the case of thermal properties of zinc(II) compound was not confirmed intermediates of the thermal decomposition. Tarykowska et al. [27] studied antioxidant activity of 4-hydroxybenzoic acid and its fluorine and hydroxy derivatives. It was prepared only a few zinc(II) 4-hydroxybenzoates.

Continuation of our studies is the preparation of the zinc(II) 4-hydroxybenzoate complexes with organic ligands such as isonicotinamide, *N*-methylnicotinamide, *N*,*N*-diethylnicotinamide, thiourea, urea, phenazone, theophylline and methyl-3-pyridylcarbamate (Scheme 1) and study of their thermal, spectral and biological properties.

Experimental

Synthesis of the compounds

Chemicals of analytical grade, $ZnCl_2$ (Fluka, Germany), $NaHCO_3$ (Centralchem, Slovakia), 4-hydroxybenzoic acid (Aldrich, Germany), methyl-3-pyridylcarbamate, phenazone (Merck, Germany), isonicotinamide (Aldrich, Germany), theophylline (Fluka, Germany), urea (Merck, Germany), *N*,*N*-diethylnicotinamide, *N*-methylnicotinamide (Acros Organics, Belgium) and thiourea (Lachema, Czech Republic), were used.

The following compounds were prepared: $[Zn(4\text{-}OHbenz)_2]{\cdot}3{,}5H_2O$ (**I**), $[Zn(4\text{-}OHbenz)_2tu_2]$ (**II**), $[Zn(4\text{-}OHbenz)_2u_2]{\cdot}3H_2O$ (**III**), $[Zn(4\text{-}OHbenz)_2phen_3]$ (**IV**), $[Zn(4\text{-}OHbenz)_2tph_2]{\cdot}2H_2O$ (**V**), $[Zn(4\text{-}OHbenz)_2mnad_3]$ (**VI**), $[Zn(4\text{-}OHbenz)_2dnad_2]$ (**VII**), $[Zn(4\text{-}OHbenz)_2inad_3]$ (**VIII**) and $[Zn(4\text{-}OHbenz)_2mpc_3]$ (**IX**).

The synthesis of the compounds may be expressed by the following equations:

$$ZnCl_2 + 2NaHCO_3 \rightarrow ZnCO_3 + 2\ NaCl + H_2CO_3 \quad (1)$$

$$ZnCO_3 + 2(4\text{-}OH\text{-}C_6H_4COOH) \rightarrow Zn(4\text{-}OH\text{-}C_6H_4COO)_2 + H_2O + CO_2 \quad (2)$$

$$Zn(4\text{-}OH\text{-}C_6H_4COO)_2 + nL \rightarrow Zn(4\text{-}OH\text{-}C_6H_4COO)_2L_n \quad (3)$$

$ZnCO_3$ was prepared by reaction of the stoichiometric amounts of $ZnCl_2$ and $NaHCO_3$ as described in Eq. 1. The reaction mixture was stirred for 1 h and filtered off. Then, the ethanol solution of carboxylic acid was added to the water suspension of $ZnCO_3$ under continual stirring and zinc(II) 4-hydroxybenzoate was formed as described in Eq. 2. A water solution of ligand (u, phen, mnad) or an ethanol solution of ligand (mpc, tph, dnad, inad) was added to the solution of zinc(II) 4-hydroxybenzoate as described in Eq. 3. The reaction mixture was reduced to a half of its volume at 80 °C and left to crystallize at room temperature. After several days, white crystals were formed.

Scheme 1 Molecular formula of selected bioactive ligands and scheme of synthesized compounds (L is ligand)

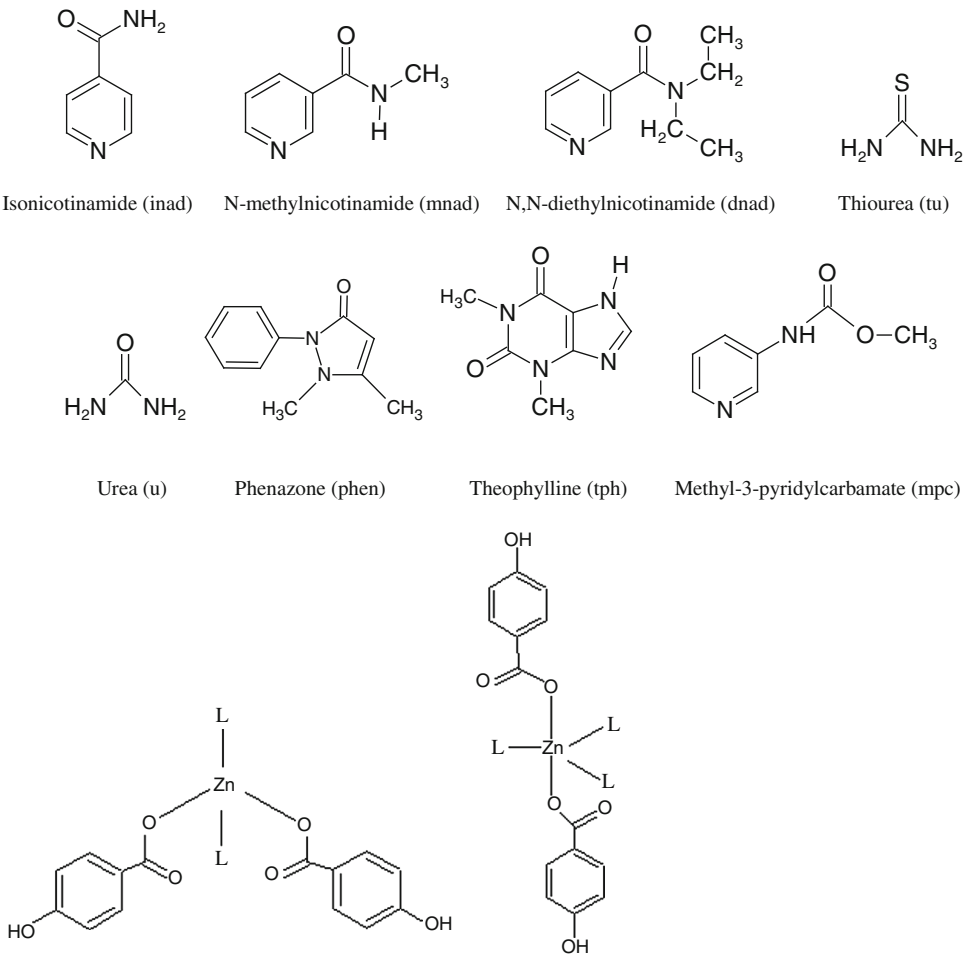

Instrumentation

Elemental (C, H, N, S) analysis of prepared compounds was determined by means of Perkin Elmer 2400 CHN analyser. The infrared spectra were recorded on AVATAR 330 FTIR Thermo Nicolet spectrophotometer in the range 4000–400 cm^{-1} using KBr pellets (2 mg of sample per 200 mg of KBr). The content of zinc was determined complexometrically using Complexone III as an agent and Eriochrome black as an indicator.

The thermal measurements of TG/DTG and DTA were carried out up to 1 200 K, heating rate at 9 K min^{-1} in an argon atmosphere by the NETZSCH STA 409 PC/PG thermoanalyser (Germany) and Perkin Elmer DSC, TGA Pyris 1 (USA). The sample was placed in ceramic crucible (25.1–34.9 mg sample). The volatile gaseous products, solid intermediate products and the final product of thermal decomposition were identified by IR spectroscopy, mass spectrometry, qualitative chemical analyses and X-ray powder diffraction method. Solid final product of the thermal decomposition was identified by X-ray powder diffraction analysis with Bruker D8 powder diffractometer (Germany). Mass spectrometer GC/MS Agilent 7890A was used for the determination of volatile products of the thermal decomposition.

Antimicrobial assay

The antibacterial activities of the studied zinc(II) 4-hydroxybenzoate complexes, 4-hydroxybenzoic acid and free ligands (*N*,*N*-diethylnicotinamide, thiourea, isonicotinamide, *N*-methylnicotinamide, urea phenazone, theophylline and methyl-3-pyridylcarbamate) were evaluated by a microdilution method using G^+ bacteria *Staphylococcus aureus* CCM 3953 and G^- bacteria *Escherichia coli* CCM 3988 [28]. The effects of these compounds on the growth of yeasts, *Candida parapsilosis,* were determined by macrodilution method in L-shapes tubes adapted for direct measurement of absorbance [29]. The cultures of bacteria (in Mueller–Hinton growth medium) and yeasts (Sabouraud's growth medium) were incubated under vigorous shaking. The effect of tested compounds on the growth of filamentous fungi *Rhizopus oryzae* CCM F-8284, *Alternaria alternata* CCM F-128 and *Microsporum gypseum* CCM F-8342 was

observed by macrodilution technique on solidified broth medium during static culturing [30, 31], and the diameters of growing fungal colonies were measured at intervals.

The studied compounds were dissolved in DMSO. Its final concentration never exceeded 1.0 vol% in either control or treated samples. Concentration of tested compounds was in the range of 0.001–2.0 mmol dm^{-3} in all experiments. The antimicrobial activity of tested compound was characterised by the IC_{50} values (concentration of a compound, which compared with the control inhibits the growth of model microorganisms to 50 %) and also by the MIC values (minimal inhibitory concentration of a compound which inhibits microbial growth by 100 %). The IC_{50} and MIC values were read from toxicity curves. MIC experiments on subculture dishes were used to assess the minimal microbicidal concentration (MMC). Subcultures were prepared separately in Petri dishes containing appropriate agar growth medium, and incubated at 30 °C for 48 h (bacteria and yeasts) and 25 °C for 96 h (filamentous fungi). The MMC value was taken as the lowest concentration which showed no visible growth of microbial colonies on the subculture dishes.

Results and discussion

The prepared compounds are white in colour, stable in air and light. The results of elemental analysis are in good agreement with the calculated ones (Table 1).

IR spectroscopy

The characteristic absorption bands in IR spectra of the prepared compounds, that provide valuable information regarding the type of functional groups, are reported in Table 2. The assignments are in accordance with the literature data [32, 33].

In the studied compounds, there were identified stretching vibrations ν(C–H) of the aromatic ring in the range 3024–3085 cm^{-1}, stretching aliphatic vibrations

Table 1 Elemental analysis of the prepared zinc(II) compounds

Compound	C/%		H/%		N/%		S/%		Zn/%	
	Exp.	Calc.	Exp.	Calc.	Exp.	Calc.	Exp.	Calc.	Exp.	Calc.
$[Zn(4\text{-}OHbenz)_2]\cdot 3{,}5H_2O$ (**I**) $C_{14}H_{17}O_{9,5}Zn$ F. W. = 402.67	41.81	41.75	3.43	4.25	–	–	–	–	16.04	16.24
$[Zn(4\text{-}OHbenz)_2tu_2]$ (**II**) $C_{16}H_{18}O_6N_4S_2Zn$ F. W. = 491.85	38.71	39.07	3.58	3.68	12.76	11.39	13.28	13.03	13.43	13.29
$[Zn(4\text{-}OHbenz)_2u_2]\cdot 3H_2O$ (**III**) $C_{16}H_{24}O_{11}N_4Zn$ F. W. = 513.77	38.58	37.40	4.51	4.71	10.83	10.91	–	–	12.93	12.72
$[Zn(4\text{-}OHbenz)_2phen_3]$ (**IV**) $C_{47}H_{46}O_9N_6Zn$ F. W. = 904.28	62.98	62.43	4.58	5.13	8.61	9.29	–	–	7.44	7.23
$[Zn(4\text{-}OHbenz)_2tph_2]\cdot 2H_2O$ (**V**) $C_{28}H_{30}O_{12}N_8Zn$ F. W. = 735.988	45.66	45.69	3.67	4.10	15.53	15.22	–	–	9.11	8.88
$[Zn(4\text{-}OHbenz)_2mnad_3]$ (**VI**) $C_{35}H_{34}O_9N_6Zn$ F. W. = 748.059	56.64	56.20	4.38	4.58	10.25	11.23	–	–	9.24	8.74
$[Zn(4\text{-}OHbenz)_2dnad_2]$ (**VII**) $C_{34}H_{38}O_8N_4Zn$ F. W. = 696.07	58.93	58.67	5.64	5.50	8.67	8.05	–	–	9.45	9.39
$[Zn(4\text{-}OHbenz)_2inad_3]$ (**VIII**) $C_{32}H_{28}O_9N_6Zn$ F. W. = 705.98	54.99	54.44	3.36	3.99	11.29	11.90	–	–	9.87	9.26
$[Zn(4\text{-}OHbenz)_2mpc_3]$ (**IX**) $C_{35}H_{34}O_{12}N_6Zn$ F. W. = 796.06	53.56	52.81	3.93	4.31	10.23	10.56	–	–	8.78	8.21

Table 2 Characteristic absorption bands ν [cm^{-1}] in IR spectra of prepared compounds

Assignment/ compound	[Zn(4-OHbenz)$_2$]·3,5H_2O	[Zn(4-OHbenz)$_2$ tu_2]	[Zn(4-OHbenz)$_2$ u_2]·3H_2O	[Zn(4-OHbenz)$_2$ $phen_3$]	[Zn(4-OHbenz)$_2$ tph_2]·2H_2O	[Zn(4-OHbenz)$_2$ $mnad_3$]	[Zn(4-OHbenz)$_2$ $dnad_2$]	[Zn(4-OHbenz)$_2$ $inad_3$]	[Zn(4-OHbenz)$_2$ mpc_3]	(4-OHbenz) Na
ν(N–H)$_{NH2,\ NHR–}$	–	3385 s, 3327 s 3375* s, 3272* s	3436 s, 3338 s 3442* s, 3346* s	–	–	3358 s, 3371* s	–	3342 s, 3371* s	3282 s, 3237* s	–
ν(C–H)$_{ar}$	3024 w	3050 w	3025 w	3066 w 3092* w	3082 w 3094* w	3074 w 3098* w	3061 m 3034* w	3080 w 3063* w	3085 w 3044* w	3072 w
ν(C–H)$_{CH3–}$	–	–	–	2995 w, 2943 w, 2987* w, 2936* w,	2993 w, 2955 w 2958*w, 2917* w	2970 w, 2924 w 2963* w, 2917* w	2991 w, 2976 w 2988* w, 2963* w	–	2956 w, 2952* w	–
ν(C=O)	–	–	1632 s	1616 s	1707 s	1651 s	1637 s	1678 s	1698 s	–
			1672* s	1655* s	1714* s	1644* s	1628* s	1666* s	1728* s	–
δ(N–H)$_{NH2,\ NHR–}$	–	1608 s 1615*s	1606 s 1627*s	–	–	1635 s 1593*s	–	1601 s 1632*s	1606 s 1616*s	–
δ(O–H)$_{H2O}$	1608 s	–	1609 s	–	1635 s	–	–	–	–	–
ν(C=C)$_{ar}$	1512 s	1508 s	1514 s	1508 w	1514 m	1514 s	1506 m	1510 m	1509 s	1519 m
ν_{as}(COO^-)	1597 s	1597 s	1567 s	1570 s	1581 s	1566 s	1578 s	1554 s	1553 s	1547 s
ν_s(COO^-)	1398 s	1379 s	1375 s	1377 s	1375 s	1383 s	1366 s	1385 s	1380 s	1416 s
Δ(COO^-)	199	218	192	193	206	183	212	169	173	131
δ_{as}(C–H)$_{CH3–}$	–	–	–	1456 m 1445* m	1448 m 1446*m	1433 m, 1439* m	1458 m, 1444* m	–	1441 s 1429* s	–
ν(C–C)$_{ar}$	1425 s	1473 s	1432 s	1495 s	1481 s	1477 s	1480 s	1510 s	1491 s	1416 s
δ(O–H)$_{ph}$	1319 m	1317 m	1318 m	1315 m	1323 m	1317 m	1315 m	1312 m	1334 m	1357 m
ν(C–OH)$_{ph}$	1246 s	1244 s	1242 s	1244 s	1238 s	1232 s	1236 s	1248 s	1239 s	1261 s
ν(C–N)$_{ar}$	–	–	–	–	–	1279 s 1317* s	1265 s 1290* s	1271 s 1291* s	1270 s 1296* s	–
δ(C–H)$_{ar}$	1011 m	1011 m	1021 m	1012 w	1012 w	1005 w	1009 w	1007 w	1027 w	1019 m
γ(C–CH)$_{ar}$	854 s	856 s	848 s	858 s	852 s	850 s	860 s	856 s	856 s	849 s
δ(COO^-)	694 m	715 m	695 m	694 m	687 m	704 s	706 s	702 s	700 s	–
ν(C=S)	–	1101 m, 1084* m	–	–	–	–	–	–	–	–
ν(Zn–O)	505 m	505 m	500 m	509 m	499 m	505 m	513 w	511 w	501 m	–
ν(Zn-N)	–	–	–	–	–	455 m	459 m	457 m	–	–

s strong, *m* medium, *w* weak, *ar* aromatic, *as* asymmetric, *s* symmetric

* Free ligands: *tu* thiourea, *u* urea, *phen* phenazone, *tph* theophylline, *mnad N*-methylnicotinamide, *dnad N,N*-diethylnicotinamide, *inad* isonicotinamide, *mpc* methyl-3-pyridylcarbamate, *ph* phenyl

ν(C–H) in the range 2924–2995 cm^{-1}, stretching vibrations ν(C–C) of the aromatic ring in the range 1425–1510 cm^{-1}, stretching vibrations ν(C–OH) in the range 1232–1248 cm^{-1} and out of plane bending vibrations γ(C–CH) of the aromatic ring in the range 848–860 cm^{-1}. In accordance with the literature data, the stretching vibrations of ν(Zn–O) are in the range 499–513 cm^{-1}.

Characteristic absorption bands of carbonyl group of ligands in the prepared compounds occur in the range 1616–1707 cm^{-1}. The strong absorption band of the carbonyl group of nicotinamide ligands in the prepared compounds [Zn(4-OHbenz)$_2$mnad$_3$] (**VI**), [Zn(4-OHbenz)$_2$dnad$_2$] (**VII**) and [Zn(4-OHbenz)$_2$inad$_3$] (**VIII**) are in 1651, 1637 and 1678 cm^{-1}, respectively, is shifted to a higher wavenumber (by 7, 9 and 12 cm^{-1}) as compared with the free ligands (ν_{mnad}(C=O) = 1644 cm^{-1}, ν_{dnad}(C=O) = 1628 cm^{-1}, ν_{inad}(C=O) = 1666 cm^{-1}). It can be explained by the fact that the pyridine nitrogen of nicotinamide ligands is in coordination with zinc atom, therefore, the electron density is shifted towards the pyridine nitrogen, leading to the shorting of bond length of the carbonyl group and shifting the stretching vibration of nicotinamide ligands *ν*(C=O) to a higher value.

On the other hand in the case of [Zn(4-OHbenz)$_2$u$_2$]·3H$_2$O (**III**), [Zn(4-OHbenz)$_2$phen$_3$] (**IV**), [Zn(4-OHbenz)$_2$tph$_2$]-2H$_2$O (**V**) and [Zn(4-OHbenz)$_2$mpc$_3$] (**IX**), the absorption band of the stretching vibration of carbonyl group ν(C=O) of ligands appeared at 1632, 1616, 1707 and 1698 cm^{-1}, respectively, exhibited a shift to lower wavenumber in comparison with free ligands (ν_u(C=O) = 1672 cm^{-1}, ν_{phen}(C=O) = 1655 cm^{-1}, ν_{tph}(C=O) = 1714 cm^{-1}, ν_{mpc}(C=O) = 1728 cm^{-1}). This phenomenon can be explained by the coordination of the carbonyl oxygen of ligands to the zinc atom, leading to the lengthening of the bond length of the carbonyl group and shifting the stretching vibration *ν*(C=O) to lower wavenumbers.

The IR spectra of the prepared compounds indicate the typical carboxylate stretching frequencies. For the asymmetric stretching vibration, $\nu_{as}(COO^-)$ is in the range 1553–1597 cm^{-1}, and for the symmetric stretching vibration, $\nu_s(COO^-)$ at 1366–1398 cm^{-1}.

On the basis of the magnitude of separation of asymmetric and symmetric stretching vibrations of carboxylate group Δ value [$\Delta = \nu_{as}(COO^-)$–$\nu_s(COO^-)$], it is possible to predict the type of coordination of carboxylate group in the complex compounds. From the literature [34, 35] it is known that for monodentate coordination of the carboxylate group, Δ value is higher than Δ value of sodium salt, and for the bidentate chelating coordination, the Δ value is lower for sodium salt. The calculated values of Δ in prepared compounds are in the range 169–218 cm^{-1}. The Δ value for sodium 4-hydroxybenzoate is 131 cm^{-1}. According to the above mentioned criteria, the carboxylate ion in these compounds is monodentate. It is in agreement with our previous studies that were correlated spectral data with solved crystal structure [35, 36].

Thermal behaviour

The results of thermal analysis of studied compounds are reported in Table 3.

*[Zn(4-OHbenz)$_2$]·3,5H$_2$O (**I**)*

The TG/DTG and DTA curves of [Zn(4-OHbenz)$_2$]·3,5H$_2$O are shown in Fig. 1. The first step of thermal decomposition begins with the release of water at 306 K (the experimental mass loss 16.11 %, the calculated mass loss 15.66 %). This is accompanied by three endothermic effects on the DTA curve at 339, 372 and 398 K. In the next two steps, hydroxybenzoate anion (*m/z*: 121) is decomposed and phenol (*m/z*: 93, 65, 39), CO_2 and CO are evolving (the experimental mass loss 63.93 %, the calculated mass loss 64.13 %). This decomposition process is accompanied by an endothermic effect on the DTA curve at 489 K and exothermic effect at 872 K. The mass fragmentation is in accordance with the literature data [37]:

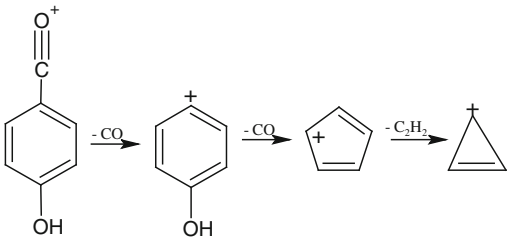

m/z 121 *m/z* 93 *m/z* 65 *m/z* 39

The final solid product of thermal decomposition was ZnO, which was confirmed by IR spectroscopy (ν_{ZnO}: 457 cm^{-1}) and X-ray powder diffraction method (Fig. 2). These results correspond with the structural data of ZnO from the literature [38]. The following reaction was proposed for the thermal decomposition:

$$[Zn(4\text{-}OHbenz)_2] \cdot 3,5H_2O \rightarrow 3,5H_2O + 2C_6H_5OH + CO_2 + CO + ZnO.$$

*[Zn(4-OHbenz)$_2$tu$_2$](**II**)*

The thermal decomposition of this compound is shown in Fig. 3. The decomposition process starts at 416 K by an endothermic effect on the DTA curve at 486 K. Above this temperature, in two steps, thiourea (*m/z*: 76, 60, 16), phenol and carbon dioxide (*m/z*: 93, 65, 44, 39) are released (the experimental mass loss 87.48 %, the calculated mass loss 86.71 %).

Table 3 Thermal decomposition of the prepared compounds

Compound	Temperature range of decomposition /K	Products of the thermal decomposition	Mass loss/%		DTA peak/effect/K
			exp.	calc.	
[Zn(4-OHbenz)$_2$].3,5 H_2O **(I)**	306-373	3,5 H_2O	16.11	15.66	339, 372, 398/endo
	373-560	phenol + CO_2	33.74 } 63.93	34.01 } 64.13	489/endo
	560-886	phenol + CO	30.19	30.12	872/exo
	R_{1200}	ZnO	19.96	20.21	
[Zn(4-OHbenz)$_2$tu$_2$] **(II)**	416-534	2 tu + phenol	52.02 } 87.48	50.08 } 86.71	486/ endo
	534-1113	phenol + 2 CO_2	35.46	36.63	870/exo
	R_{1200}	Zn	12.52	13.29	
[Zn(4-OHbenz)$_2$u$_2$].3H_2O **(III)**	334-455	3 H_2O	10.38	10.32	365, 410/endo
	455-675	2 u + 2 phenol	59.99	60.02	-
	675-1104	2CO_2	17.10	17.12	870/endo
	R_{1200}	Zn	12.53	12.54	
[Zn(4-OHbenz)$_2$phen$_3$] **(IV)**	323-659	3 phen + phenol + CO_2	78.33 } 93.13	77.62 } 92.79	-
	659-929	phenol + CO_2	14.80	15.17	1024/exo
	R_{1200}	Zn	6.87	7.21	
[Zn(4-OHbenz)$_2$tph$_2$].2H_2O **(V)**	348-452	2 H_2O	4.38	4.79	447/endo
	452-591	2 tph	48.56	48.79	496/endo
	591-691	phenol + CO_2	18.62 } 38.32	18.77 } 37.54	596/endo
	691-1002	phenol + CO_2	19.70	18.77	809, 1008/endo, exo
	R_{1200}	Zn	8.74	8.88	
[Zn(4-OHbenz)$_2$mnad$_3$] **(VI)**	513-589	3 mnad + phenol + CO_2	72.94 } 91.28	72.89 } 91.26	523, 562/ endo
	589-1102	phenol + CO_2	18.34	18.37	806/exo
	R_{1200}	Zn	8.72	8.74	
[Zn(4-OHbenz)$_2$dnad$_2$] **(VII)**	451-569	2 dnad + phenol + CO_2	71.01 } 90.82	71.05 } 90.77	542/endo
	569-1102	phenol + CO_2	19.81	19.72	866/exo
	R_{1200}	Zn	9.18	9.23	
[Zn(4-OHbenz)$_2$inad$_3$] **(VIII)**	340-569	3 inad + 2 CO_2	64.27	64.18	520, 548/endo
	569-856	2 phenol	26.53	26.60	774, 813/exo
	R_{1200}	Zn	9.20	9.22	
[Zn(4-OHbenz)$_2$mpc$_3$] **(IX)**	410-524	3 mpc	58.11	57.34	441/endo
	524-1016	2 phenol + 2 CO_2	34.88	34.70	821/exo
	R_{1200}	Zn	7.01	7.96	

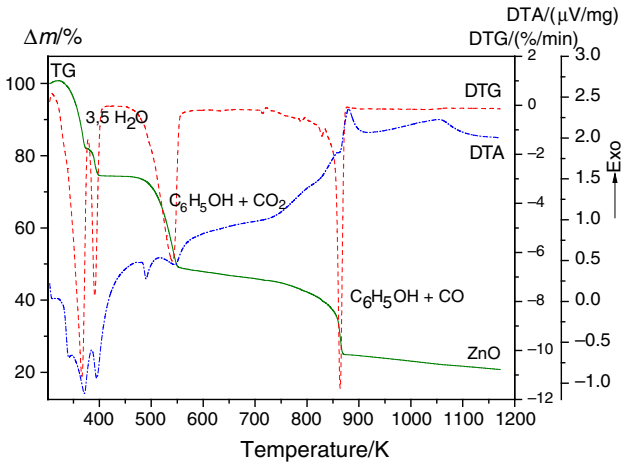

Fig. 1 TG/DTG and DTA curves of [Zn(4-OHbenz)$_2$]·3,5H_2O (I)

In the solid intermediate heated up to 534 K was confirmed the release of thiourea by IR spectroscopy (ν(N–H) = 3385, 3327 cm^{-1}, δ(N–H) = 1608 cm^{-1}, ν(C=S) = 1101 cm^{-1} were missing). The fragmentation of thiourea is as follows:

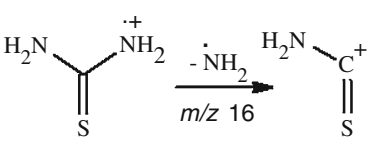

m/z 76 *m/z* 60

The final solid product of thermal decomposition was zinc (the experimental residue 12.52 %, the calculated residue 13.29 %), which was confirmed by X-ray powder diffraction method (Fig. 2). Obtained results correspond

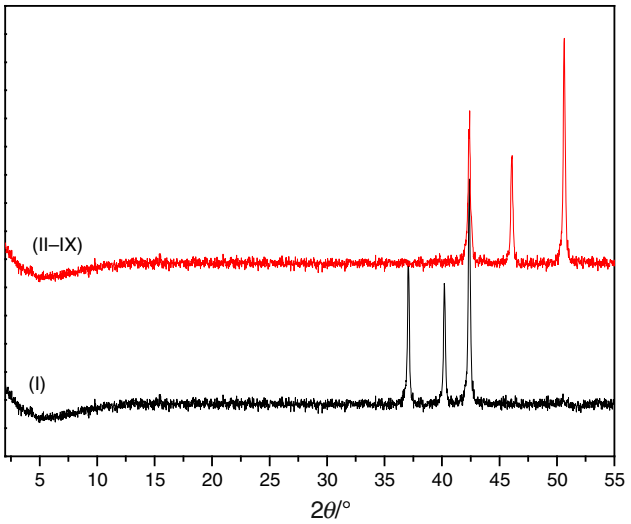

Fig. 2 Results of powder diffractometry for final product of thermal decomposition for compounds **I–IX**

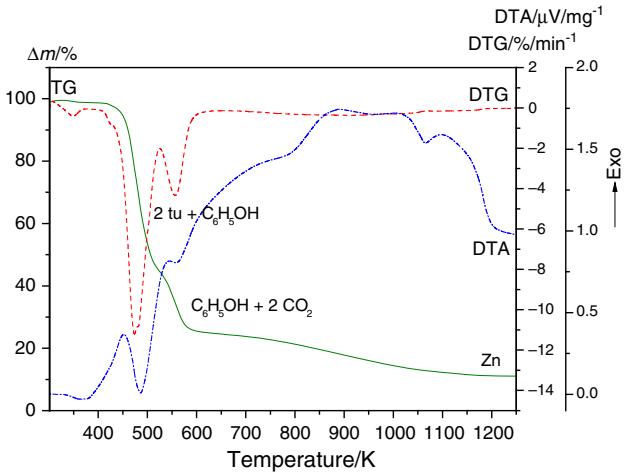

Fig. 3 TG/DTG and DTA curves of $[Zn(4\text{-}OHbenz)_2tu_2]$ (**II**)

with the structural data of zinc from the literature [38]. The following reaction was proposed for the thermal decomposition:

$$[Zn(4\text{-}OHbenz)_2tu_2] \rightarrow 2tu + 2C_6H_5OH + 2CO_2 + Zn.$$

*$[Zn(4\text{-}OHbenz)_2u_2]\cdot 3H_2O$ (**III**)*

As it can be seen from Fig. 4, the thermal decomposition of this compound starts with dehydration from 334 K (the experimental mass loss 10.38 %, the calculated mass loss 10.32 %), which is accompanied by a double endothermic effect on the DTA curve at 365 and 410 K. Then, in the temperature range 455–675 K, urea (*m/z*: 60, 44, 16) and

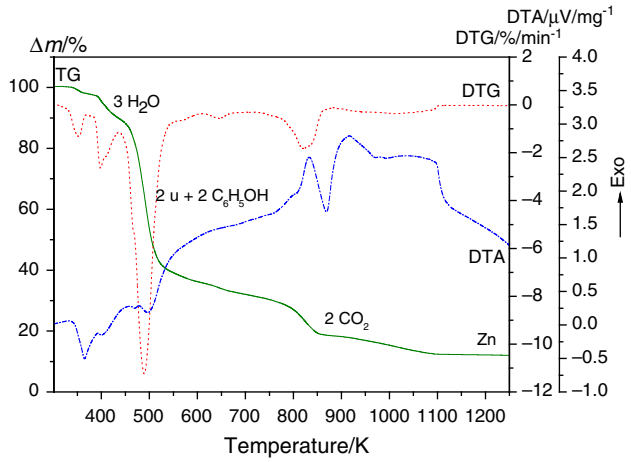

Fig. 4 TG/DTG and DTA curves of $[Zn(4\text{-}OHbenz)_2u_2]\cdot 3H_2O$ (**III**)

phenol (*m/z*: 93, 65, 39) are evolved (the experimental mass loss 59.99 %, the calculated mass loss 60.02 %). The release of urea was confirmed by IR spectroscopy heated up to 675 K in the solid intermediate. The characteristic absorption bands of urea were missing (ν(N–H) = 3436, 3338 cm^{-1}, ν(C=O) = 1632 cm^{-1}, δ(N–H) = 1606 cm^{-1}). The fragmentation of urea is as follows:

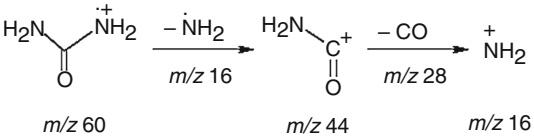

This fragmentation is in accordance with the literature [37, 39]. In the temperature range 675–1104 K, carbon dioxide (*m/z*: 44) is liberated (the experimental mass loss 17.10 %, the calculated mass loss 17.12 %). This process was accompanied by an endothermic effect on the DTA curve at 870 K.

The final solid product of thermal decomposition was zinc (the experimental residue 12.53 %, the calculated residue 12.54 %), which was confirmed by X-ray powder diffraction method (Fig. 2). These results correspond with the structural data of zinc from the literature [38]. The thermal decomposition is expressed by the following equation:

$$[Zn(4\text{-}OHbenz)_2u_2]\cdot 3H_2O \rightarrow 3H_2O + 2u + 2C_6H_5OH + 2CO_2 + Zn.$$

*$[Zn(4\text{-}OHbenz)_2phen_3]$(**IV**)*

The thermal decomposition of phenazone compound is shown in Fig. 5. During decomposition, phenazone (*m/z*: 188, 173, 96, 56), phenol (*m/z*: 93, 65, 39) and carbon dioxide (*m/z*: 44) are evolved (the experimental

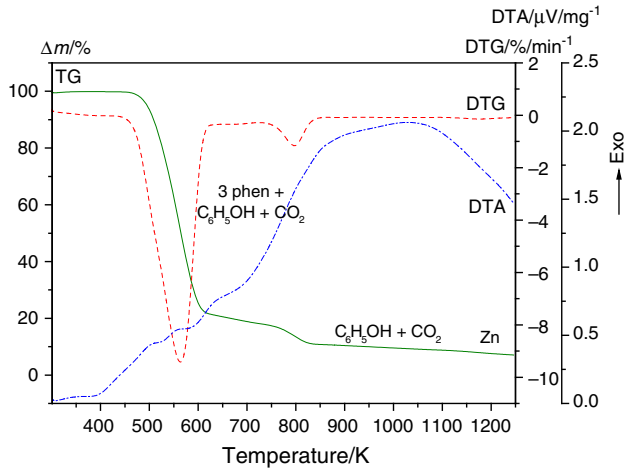

Fig. 5 TG/DTG and DTA curves of $[Zn(4\text{-}OHbenz)_2phen_3]$ (**IV**)

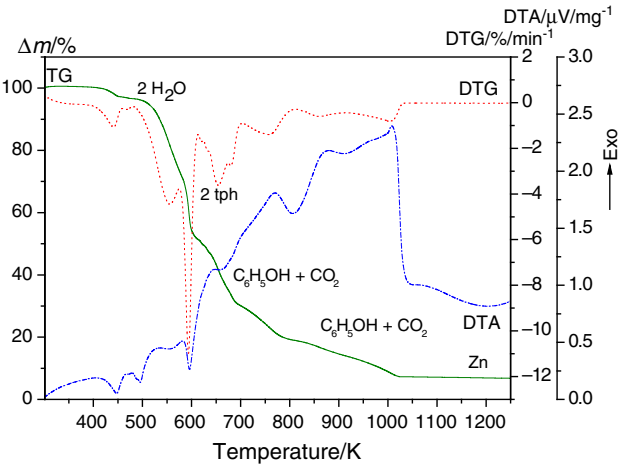

Fig. 6 TG/DTG and DTA curves of $[Zn(4\text{-}OHbenz)_2tph_2]\cdot 2H_2O$ (**V**)

mass loss 93.13 %, the calculated mass loss 92.79 %). The release of phenazone up to 659 K was confirmed by IR spectrum of the solid intermediate product, where the absorption bands of phenazone were missing (ν(C–H)$_{ar}$ = 3066 cm^{-1}, ν(C–H)$_{CH3-}$ = 2995, 2943 cm^{-1}, ν(C=O) = 1616 cm^{-1}, δ_{as}(C–H)$_{CH3-}$ = 1456 cm^{-1}). The proposed fragmentation of phenazone is shown on the following scheme:

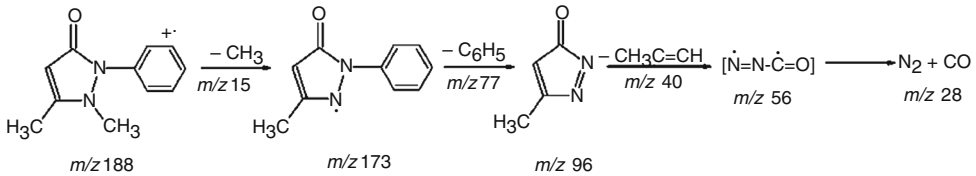

This fragmentation corresponds with the literature data [37, 39]. The final solid product of thermal decomposition was zinc (the experimental residue 6.87 %, the calculated residue 7.21 %), which was confirmed by X-ray powder diffraction method (Fig. 2). These results correspond with the structural data of zinc from the literature [38]. The following reaction is proposed for the thermal decomposition:

$$[Zn(4\text{-}OHbenz)_2phen_3] \rightarrow 3phen + 2C_6H_5OH + 2CO_2 + Zn.$$

[Zn(4-OHbenz)$_2$tph$_2$]·2H$_2$O (V)

The compound is stable up to 348 K (Fig. 6). Release of water takes place above this temperature (the experimental mass loss 4.38 %, the calculated mass loss 4.79 %). The thermal decomposition of an anhydrous product may be characterised as a several step reaction in temperature range from 452 to 1002 K. The first theophylline is released (*m/z*: 180, 123, 95, 66) (the experimental mass loss 48.56 %, the calculated mass loss 48.79 %). This fragmentation is shown on the following scheme:

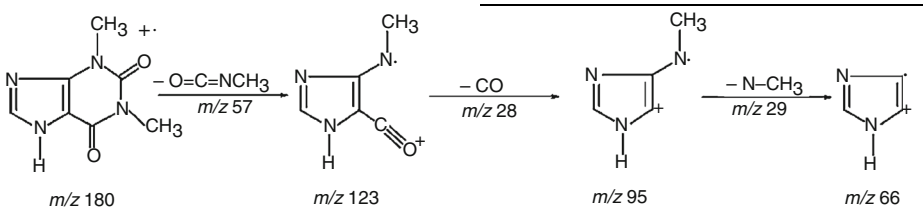

Similar theophylline fragments were obtained so as in the case of chlorobenzoate compound with theophylline [35, 37]. In the solid intermediate heated up to 591 K, the IR absorption bands of theophylline were missing (ν(C–H)$_{ar}$ = 3082 cm^{-1}, ν(C–H)$_{CH3-}$ = 2993, 2955 cm^{-1}, ν(C=O) = 1707 cm^{-1}, δ_{as}(C–H)$_{CH3-}$ = 1448 cm^{-1}). In the next steps, hydroxybenzoate anion (*m/z*: 121) is decomposed, and phenol and carbon dioxide (*m/z*: 93, 65, 44, 39) are released (the experimental mass loss 38.32 %, the calculated mass loss 37.54 %).

The final solid product of thermal decomposition was zinc (the experimental residue 8.74 %, the calculated residue 8.88 %). It was proved by X-ray powder diffraction method (Fig. 2), which results correspond with the structural data of zinc from the literature [38]. The following reaction is proposed for the thermal decomposition:

$$[\mathrm{Zn(4\text{-}OHbenz)_2tph_2}]\cdot 2\mathrm{H_2O} \rightarrow 2\mathrm{H_2O} + 2\mathrm{tph} + 2\mathrm{C_6H_5OH} + 2\mathrm{CO_2} + \mathrm{Zn}.$$

*[Zn(4-OHbenz)$_2$mnad$_3$] (**VI**)*

The thermal decomposition of [Zn(4-OHbenz)$_2$mnad$_3$] is shown in Fig. 7. The compound is melting at 389 K. The decomposition starts at 513 K, and *N*-methylnicotinamide (*m/z*: 136, 107, 79, 52), phenol and carbon dioxide (*m/z*: 93, 65, 44, 39) are evolved (the experimental mass loss 91.28 %, the calculated mass loss 91.26 %). These decomposition processes are accompanied by a double endothermic effect at 523 and 562 K and exothermic effect at 806 K. The fragmentation of *N*-methylnicotinamide is as follows:

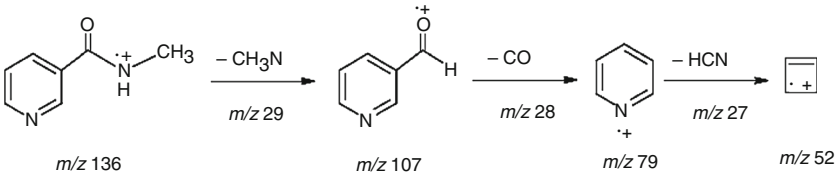

The fragmentation is in accordance with the literature data [37, 39]. In the IR spectrum of the solid intermediate product heated up to 589 K, the absorption bands of *N*-methylnicotinamide were missing (ν(N–H) = 3358 cm^{-1}, ν(C–H)$_{ar}$ = 3074 cm^{-1}, ν(C–H)$_{CH3-}$ = 2970, 2924 cm^{-1}, ν(C=O) = 1651 cm^{-1}, δ(N–H) = 1635 cm^{-1}, δ_{as}(C–H)$_{CH3-}$ = 1433 cm^{-1}, ν(C–N)$_{ar}$ = 1279 cm^{-1}).

The final solid product of the thermal decomposition was zinc (the experimental residue 8.72 %, the calculated residue 8.74 %), which was confirmed by X-ray powder diffraction method (Fig. 2). Observed results correspond with the structural data of zinc from the literature [38]. The

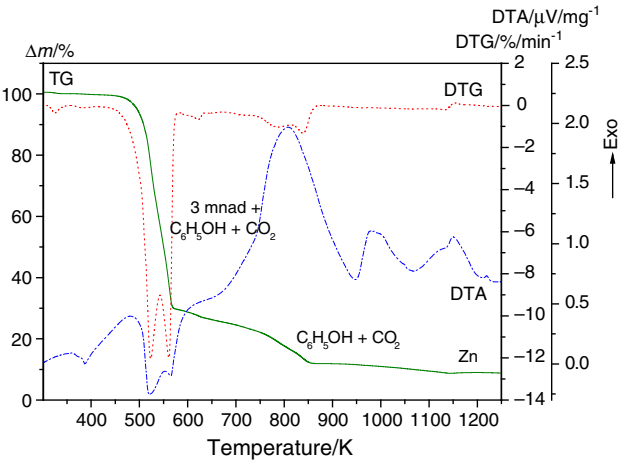

Fig. 7 TG/DTG and DTA curves of [Zn(4-OHbenz)$_2$mnad$_3$] (VI)

following equation for the thermal decomposition can be proposed as follows:

$$[\mathrm{Zn(4\text{-}OHbenz)_2mnad_3}] \rightarrow 3\mathrm{mnad} + 2\mathrm{C_6H_5OH} + 2\mathrm{CO_2} + \mathrm{Zn}.$$

*[Zn(4-OHbenz)$_2$dnad$_2$](**VII**)*

The thermogravimetric curve of this compound (Fig. 8) shows that the complex is stable up to 451 K. On heating above this temperature, thermal decomposition takes place. Then *N*,*N*-diethylnicotinamide (*m/z*: 177, 107, 79, 52) is evolved, hydroxybenzoate anion (*m/z*: 121) is decomposed and phenol and carbon dioxide (*m/z*: 93, 65, 44, 39) are evolved (the experimental mass loss 90.82 %, the calculated mass loss 90.77 %).

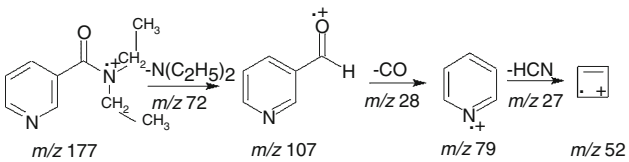

Fragmentation is in accordance with the literature data [37, 39]. In the IR spectrum of the solid intermediate product heated up to 569 K, the absorption bands of *N*,*N*-diethylnicotinamide were missing (ν(C–H)$_{ar}$ = 3061 cm^{-1},

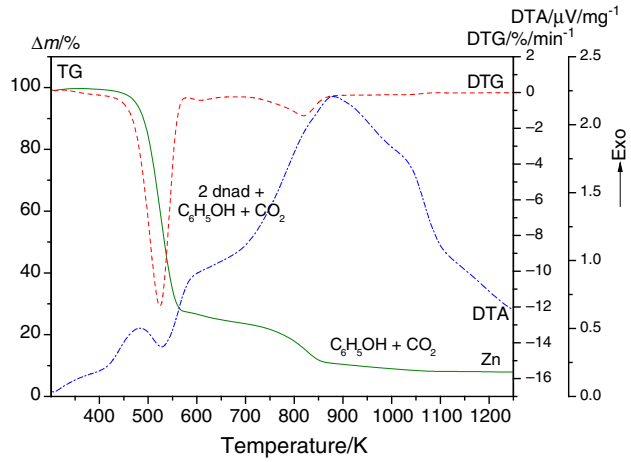

Fig. 8 TG/DTG and DTA curves of $[Zn(4\text{-}OHbenz)_2dnad_2]$ (**VII**)

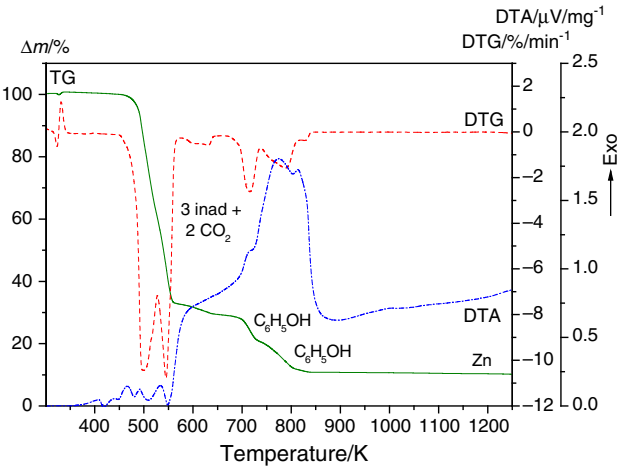

Fig. 9 TG/DTG and DTA curves of $[Zn(4\text{-}OHbenz)_2inad_3]$ (**VIII**)

$\nu(C–H)_{CH3–} = 2991,\ 2976\ cm^{-1}$, $\nu(C{=}O) = 1637\ cm^{-1}$, $\delta_{as}(C–H)_{CH3–} = 1458\ cm^{-1}$, $\nu(C–N)_{ar} = 1265\ cm^{-1}$).

The final solid product of thermal decomposition was zinc (the experimental mass loss 9.18 %, the calculated mass loss 9.23 %), which was confirmed by X-ray powder diffraction method (Fig. 2). These results correspond with the structural data of zinc from the literature [38]. In the case of thermal decomposition, in the air, zinc oxide is the final product of the thermal decomposition [26]. The following decomposition reaction is proposed for the decomposition process:

$$[Zn(4\text{-}OHbenz)_2dnad_2] \rightarrow 2dnad + 2C_6H_5OH + 2CO_2 + Zn.$$

*[Zn(4-OHbenz)$_2$inad$_3$](**VIII**)*

From Fig. 9, it is followed that this compound is stable up to 340 K. Above this temperature, isonicotinamide (*m/z*: 122, 106, 78, 51) and carbon dioxide (*m/z*: 44) are evolved. The experimental mass loss is 64.27 %, the calculated mass loss is 64.18 %. In the temperature range 569–856 K, hydroxybenzoate anion (*m/z*: 121) is decomposed and phenol (*m/z*: 93, 65, 39) is evolved in two steps (the experimental mass loss 26.53 %, the calculated mass loss 26.60 %).

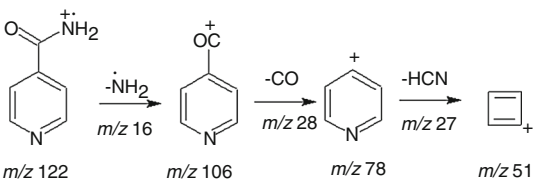

This fragmentation is in accordance with the literature [37, 39]. In the IR spectrum of solid intermediate product heated up to 569 K, the absorption bands of isonicotinamide were missing (ν(N–H) = 3342 cm^{-1}, $\nu(C–H)_{ar} = 3080\ cm^{-1}$, $\nu(C{=}O) = 1678\ cm^{-1}$, δ(N–H) = 1601 cm^{-1}, $\nu(C–N)_{ar} = 1271\ cm^{-1}$).

The final product of thermal decomposition was zinc (the experimental residue 9.20 %, the calculated residue 9.22 %), which was confirmed by X-ray powder diffraction method (Fig. 2), which results correspond with the structural data of zinc from the literature [38]. We proposed the following reaction of thermal decomposition:

$$[Zn(4\text{-}OHbenz)_2inad_3] \rightarrow 3inad + 2C_6H_5OH + 2CO_2 + Zn.$$

*[Zn(4-OHbenz)$_2$mpc$_3$](**IX**)*

As it can be seen from Fig. 10, the compound is stable up to 410 K. On heating above this temperature, thermal decomposition takes place. The release of methyl-3-pyridylcarbamate (*m/z*: 152, 120, 92, 78, 66, 51, 39) is observed on the TG curve in the temperature range 410–524 K (the experimental mass loss 58.11 %, the calculated mass loss 57.34 %). In the IR spectrum of the solid intermediate heated up to 524 K, the absorption bands of ligand were missing (ν(N–H) = 3282 cm^{-1}, $\nu(C–H)_{ar} = 3085\ cm^{-1}$, $\nu(C–H)_{CH3–} = 2956\ cm^{-1}$, $\nu(C{=}O) = 1698\ cm^{-1}$, δ(N–H) = 1606 cm^{-1}, $\delta_{as}(C–H)_{CH3–} = 1441\ cm^{-1}$, $\nu(C–N)_{ar} = 1270\ cm^{-1}$). Fragmentation of methyl-3-pyridylcarbamate is as follows:

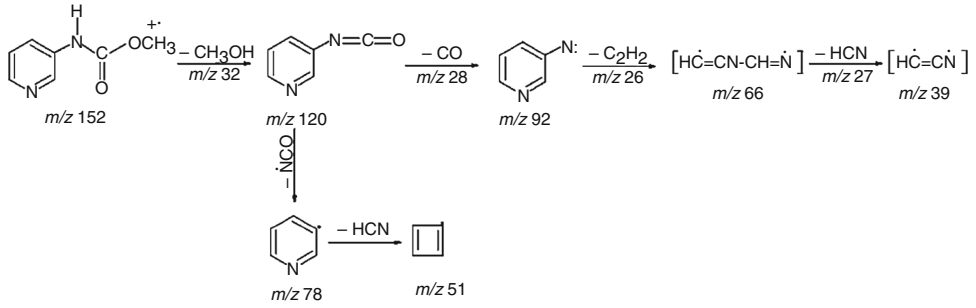

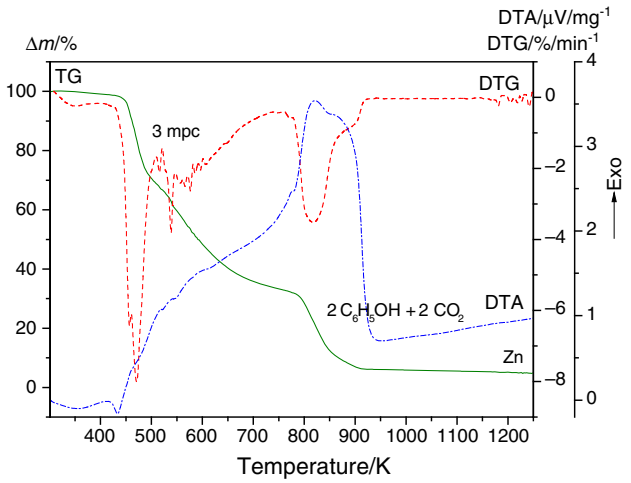

Fig. 10 TG/DTG and DTA curves of $[Zn(4\text{-}OHbenz)_2mpc_3]$ (**IX**)

These methyl-3-pyridylcarbamate fragments were proved in the case of chlorobenzoate compound with methyl-3-pyridylcarbamate [35, 37]. In the last step of thermal decomposition, in the temperature range 524–1016 K, phenol and carbon dioxide (*m/z*: 93, 65, 44, 39) are evolved (the experimental mass loss 34.88 %, the calculated mass loss 34.70 %).

The final solid product of thermal decomposition was zinc (the experimental residue 7.01 %, the calculated residue 7.96 %), which was proved by X-ray powder diffraction method (Fig. 2). Obtained results correspond with the structural data of zinc from the literature [38]. The following reaction is proposed for thermal decomposition:

$$[Zn(4\text{-}OHbenz)_2mpc_3] \rightarrow 3mpc + 2C_6H_5OH + 2CO_2 + Zn.$$

Antimicrobial activity

The results of quantitative determination of antimicrobial activity of new hydroxybenzoate zinc(II) compounds, 4-hydroxybenzoic acid and N-donor ligands were characterised by IC_{50} and MIC values. These values which we obtained on the basis of toxicity curves are listed in Table 4 and Fig. 11.

4-Hydroxybenzoic acid and ligands (urea, thiourea, methyl-3-pyridylcarbamate, phenazone, theophylline, *N*-methylnicotinamide, *N,N*-diethylnicotinamide, isonicotinamide) were antimicrobially inactive (IC_{50}, MIC > 2 mmol dm^{-3}).

The highest growth inhibition of the prepared zinc benzoato complexes has been recorded against G^+ *S. aureus*. Whereas, the presence of free 4-hydroxybenzoic acid in the highest used concentration (2 mmol dm^{-3}) has not been recorded growth inhibition of *S. aureus*. The results achieved clearly demonstrate that the presence of zinc in complexes has resulted in an increase of the antibacterial activity. Unlike, for free acid (**X**) IC_{50} and MIC were higher 2 mmol dm^{-3}, total (100 %) growth inhibition of *S. aureus* by tested zinc complexes, we observed at concentration 0.5 mmol dm^{-3} with bacteriostatical activity. On the basis of a comparison of IC_{50} values, it could be concluded that the presence of urea, thiourea, theophylline and N-methylnicotinamide ligands in complexes led to an increase their antibacterial activity (Table 4). Salicylates and halogenosalicylates have lower efficiency [20–22].

4-Hydroxybenzoic acid and prepared zinc complexes did not affect growth of G^- *E. coli* (IC_{50} and MIC > 2 mmol dm^{-3}) except compounds with theophylline and methyl-3-pyridylcarbamate (**V, IX**) (IC_{50} = 0.82 and 1.7 mmol dm^{-3}, respectively, MIC > 2 mmol dm^{-3}). Chlorosalicylates with tph [20, 21] and mpc [22] have higher efficiency (Table 4).

Antifungal activity of tested zinc complex compounds was weak. 4-Hydroxybenzoic acid at the highest used concentration (2 mmol dm^{-3}) did not affect the growth of model yeasts *C. parapsilosis* and filamentous fungi *R. oryzae, A. alternata* and *M. gypseum* (IC_{50} and MIC > 2 mmol dm^{-3}). The presence of zinc in tested compounds increased antiyeast effect. 100 % growth inhibition of *C. parapsilosis* was observed at concentration 1 mmol dm^{-3} for all zinc complexes with fungistatical effect on the yeasts cells. Prepared zinc(II) 4-hydroxybenzoates have higher efficiency towards yeast *C. parapsilosis* (IC_{50} = 0.25–0.63 mmol dm^{-3}) than

Table 4 Antimicrobial activity of Zn(II) compounds characterised by numerical values of IC_{50} and MIC (mmol dm^{-3})

Compound	Bacteria				Yeasts		Filamentous fungi						Ref.
	S. aureus		*E. coli*		*C. parapsilosis*		*R. oryzae*		*A. alternata*		*M. gypseum*		
	IC_{50}	MIC	IC_{50}	MIC	IC_{50}	MIC	IC_{50}	MIC	IC_{50}	MIC	IC_{50}	MIC	
$[Zn(4\text{-}OHbenz)_2]\cdot 3{,}5H_2O$ (**I**)	0.028	0.5[a]	>2	>2	0.25	1[a]	2.0	>2	1.20	>2	>2	>2	
$[Zn(2\text{-}OHbenz)_2]\cdot 2H_2O$	0.63	2[a]	1.30	3[a]			>3	>3	2.00	>3	1.20	2[b]	[20]
$[Zn(4\text{-}Cl\text{-}2\text{-}OHbenz)_2(H_2O)_2]$	0.58	2[a]	0.78	2[a]			1.60	3[b]	1.00	2[b]	1.00	2[b]	[21]
$[Zn(5\text{-}Cl\text{-}2\text{-}OHbenz)_2]\cdot 2H_2O$	0.51	2[a]	0.70	3[a]			>3	>3	1.00	>3	0.60	2[b]	[20]
$[Zn(4\text{-}OHbenz)_2tu_2]$ (**II**)	0.024	0.5[a]	>2	>2	0.25	1[a]	>2	>2	1.80	>2	>2	>2	
$[Zn(4\text{-}OHbenz)_2u_2]\cdot 3H_2O$ (**III**)	0.024	0.5[a]	>2	>2	0.40	1[a]	>2	>2	1.40	>2	>2	>2	
$[Zn(2\text{-}OHbenz)_2u_2]\cdot 2H_2O$	0.61	>3	1.00	3[a]			>3	>3	1.80	3[b]	2.10	>3	[20]
$[Zn(5\text{-}Cl\text{-}2\text{-}OHbenz)_2u_4]\cdot H_2O$	0.66	2[a]	1.50	>3			>3	>3	2.50	>3	1.20	2[b]	[20]
$[Zn(4\text{-}OHbenz)_2phen_3]$ (**IV**)	0.06	0.5[a]	>2	>2	0.30	1[a]	>2	>2	1.80	>2	>2	2[b]	
$[Zn(5\text{-}Cl\text{-}2\text{-}OHbenz)_2phen_2]$	0.50	3[a]	0.52	>3			2.50	>3	1.70	>3	1.40	3[b]	[22]
$[Zn(4\text{-}OHbenz)_2tph_2]\cdot 2H_2O$ (**V**)	0.024	0.5[a]	0.82	>2	0.25	1[a]	>2	>2	>2	>2	>2	>2	
$[Zn(2\text{-}OHbenz)_2tph_2]\cdot 2H_2O$	0.61	2[a]	2.10	3[a]			>3	>3	2.20	>3	1.30	3[b]	[20]
$[Zn(4\text{-}Cl\text{-}2\text{-}OHbenz)_2(H_2O)_4]\cdot 2tph\cdot 2H_2O$	1.30	2	1.00	2			2.50	>3	1.60	3[a]	1.20	2[b]	[21]
$[Zn(5\text{-}Cl\text{-}2\text{-}OHbenz)_2tph_2]\cdot 4H_2O$	0.56	2[a]	0.60	3[a]			2.40	>3	1.80	>3	1.00	3[b]	[20]
$[Zn(4\text{-}OHbenz)_2mnad_3]$ (**VI**)	0.021	0.5[a]	>2	>2	0.60	1[a]	1.7	>2	1.00	>2	1.6	>2	
$[Zn(4\text{-}Cl\text{-}2\text{-}OHbenz)_2mnad_2(H_2O)_2]$	0.54	3[a]	0.50	3[a]			1.20	>3	1.50	3[a]	1.00	3[b]	[21]
$[Zn(5\text{-}Cl\text{-}2\text{-}OHbenz)_2mnad_2(H_2O)_2]$	0.50	3[a]	1.10	3[a]			2.00	>3	2.50	>3	2.50	>3	[21]
$[Zn(4\text{-}OHbenz)_2dnad_2]$ (**VII**)	0.052	0.5 [a]	>2	>2	0.59	1[a]	>2	>2	1.6	>2	>2	>2	
$[Zn(4\text{-}Cl\text{-}2\text{-}OHbenz)_2dnad_2(H_2O)_2]$	0.51	3[b]	0.53	>3			2.00	>3	1.30	3[b]	2.00	3[b]	[21]
$[Zn(5\text{-}Cl\text{-}2\text{-}OHbenz)_2dnad_2(H_2O)_2]$	0.80	>3	0.68	3[a]			–	–	3.00	>3	>3	>3	[21]
$[Zn(4\text{-}OHbenz)_2inad_3]$ (**VIII**)	0.052	0.5[a]	>2	>2	0.30	1[a]	>2	>2	1.5	>2	>2	>2	
$[Zn(4\text{-}Cl\text{-}2\text{-}OHbenz)_2inad_2]$	0.52	3[a]	0.51	3[a]			1.70	>3	1.40	2[a]	1.30	2[a]	[21]
$[Zn(5\text{-}Cl\text{-}2\text{-}OHbenz)_2inad_2(H_2O)]$	0.55	3[a]	0.51	3[a]			2.70	>3	2.40	>3	>3	>3	[21]
$[Zn(4\text{-}OHbenz)_2mpc_3]$ (**IX**)	0.050	0.5[a]	1.7	>2	0.63	1[a]	1.6	>2	1.4	>2	>2	>2	
$[Zn(4\text{-}Cl\text{-}2\text{-}OHbenz)_2mpc_4]$	0.20	2[a]	0.30	2[a]			1.30	2[b]	1.00	>2	1.20	2[b]	[22]
$[Zn(5\text{-}Cl\text{-}2\text{-}OHbenz)_2mpc_2]$	0.21	2[a]	0.30	2[a]			2.00	>3	1.50	>3	1.30	3[b]	[22]
4-OHbenzoic acid (**X**)	>2	>2	>2	>2	>2	>2	>2	>2	>2	>2	>2	>2	
tu, u, phen, tph, mnad, dnad, inad, mpc	>2	>2	>2	>2	>2	>2	>2	>2	>2	>2	>2	>2	

[a] Microbiostatic effect

[b] Microbicidal effect

filamentous fungi. The highest efficiency towards *C. parapsilosis* has compounds (**I**, **II**, **V**) ($IC_{50} = 0.25$ mmol dm^{-3}).

4-Hydroxybenzoic acid and zinc complexes did not affect growth of *Rhizopus oryzae* (IC_{50}, MIC > 2 mmol dm^{-3}), except compounds with *N*-methylnicotinamide and methyl-3-pyridylcarbamate (**VI, IX**) ($IC_{50} = 1.7$ and 1.6 mmol dm^{-3}, respectively, MIC > 2 mmol dm^{-3}). The presence of zinc in complexes caused increased of antifungal activity of *Alternaria alternata*. Zinc(II) 4-hydroxybenzoates have the highest efficiency from filamentous fungi towards *A. alternata* ($IC_{50} = 1.0$–1.8 mmol dm^{-3}). They are less effective towards *R. oryzae* and *M. gypseum*. Compound with mnad (**VI**) affects the growth of *R. oryzae* and *M. gypseum* and compound with mpc (**IX**) affects the growth of *R. oryzae*. Other prepared compounds are biologically inactive. It was found by comparison that salicylates and halogenosalicylates [20–22] are more effective towards *M. gypseum* than zinc(II) 4-hydroxybenzoates. It was observed various biological activity depending on the position of chlorine and type of ligand. On the basis of a comparison of the IC_{50} values for prepared zinc complex compounds: $IC_{50} = 1$–2 mmol dm^{-3}, MIC > 2 mmol dm^{-3}(see Table 4), it can be concluded that presence of ligands except compound (**VI**) with N-methylnicotinamide ($IC_{50} = 1.0$ mmol dm^{-3}, MIC > 2 mmol dm^{-3}) caused decrease of inhibitory activity towards $[Zn(4\text{-}OHbenz)_2]\cdot 3{,}5H_2O$ (**I**) ($IC_{50} = 1.2$ mmol dm^{-3}, MIC > 2 mmol dm^{-3}). 4-Hydroxybenzoic

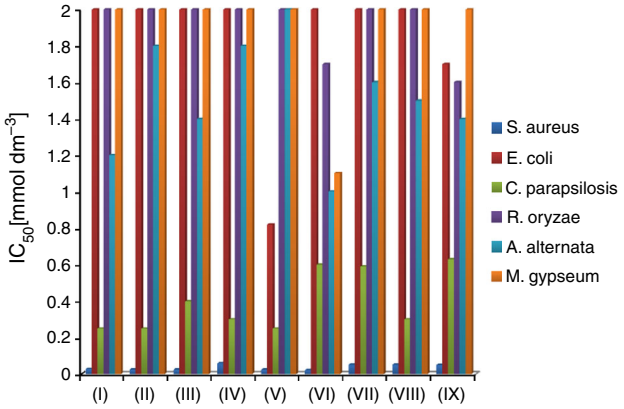

Fig. 11 Antimicrobial efficiency of compounds against bacteria, yeasts and filamentous fungi, $[Zn(4\text{-}OHbenz)_2]\cdot 3{,}5H_2O$ (**I**), $[Zn(4\text{-}OHbenz)_2tu_2]$ (**II**), $[Zn(4\text{-}OHbenz)_2u_2]\cdot 3H_2O$ (**III**), $[Zn(4\text{-}OHbenz)_2phen_3]$ (**IV**), $[Zn(4\text{-}OHbenz)_2tph_2]\cdot 2H_2O$ (**V**), $[Zn(4\text{-}OHbenz)_2mnad_3]$ (**VI**), $[Zn(4\text{-}OHbenz)_2dnad_2]$ (**VII**), $[Zn(4\text{-}OHbenz)_2inad_3]$ (**VIII**) and $[Zn(4\text{-}OHbenz)_2mpc_3]$ (**IX**)

acid and its zinc complexes except compound (**VI**) with *N*-methylnicotinamide ($IC_{50} = 1.6$ mmol dm^{-3}, MIC $>$ 2 mmol dm^{-3}) did not affect growth of dermatophytic *M. gypseum* (IC_{50} and MIC $>$ 2 mmol dm^{-3}).

Conclusions

The thermal decomposition of the studied compounds is a multistep process. During the thermal decomposition of the prepared compounds, the organic ligand and volatile products (phenol, carbon dioxide or carbon monoxide) were evolved. The final solid product of thermal decomposition is zinc or zinc oxide. The thermal stability of studied compounds decreases in the following order:

$$\underset{513\ K}{[Zn(4\text{-}OHbenz)_2mnad_3]} > \underset{451\ K}{[Zn(4\text{-}OHbenz)_2dnad_2]} > \underset{416\ K}{[Zn(4\text{-}OHbenz)_2tu_2]} > \underset{410\ K}{[Zn(4\text{-}OHbenz)_2mpc_3]} > \underset{348\ K}{[Zn(4\text{-}OHbenz)_2tph_2]\cdot 2H_2O} > \underset{340\ K}{[Zn(4\text{-}OHbenz)_2inad_3]} > \underset{334\ K}{[Zn(4\text{-}OHbenz)_2u_2]\cdot 3H_2O} > \underset{323\ K}{[Zn(4\text{-}OHbenz)_2phen_3]} > \underset{306\ K}{[Zn(4\text{-}OHbenz)_2]\cdot 3{,}5H_2O}$$

On the basis of measured IR spectra and the values of separation Δ, we assume monodentate coordination of carboxylate group in the prepared complex compounds.

In general, it could be concluded that obtained results show that the presence of zinc(II) ion in complexes led to the increase of the inhibitory activity on the growth of model bacteria, yeasts and filamentous fungi in comparison with free 4-hydroxybenzoic acid. The highest antifungal activity towards *A. alternata* and antibacterial activity towards *S. Aureus* was observed in *N*-methylnicotinamide complex (**VI**). Biological activity of the prepared compounds decreased in the following order: bacteria $>$ yeasts $>$ filamentous fungi.

Acknowledgements The financial support of VVGS-PF-2013-85 for this study is gratefully acknowledged. The authors thanks to V. Jorík and K. Matelková for XRD powder diffraction measurements.

References

1. Kendrick MJ, May MT, Plishka MJ, Robinson KD. Metals in biological systems. London: Ellis Horwood Limited; 1992.
2. Van Hoogdalem EJ. Transdermal absorption of topical anti-acne agents in man; review of clinical pharmacokinetic data. J Eur Acad Dermatol Venereol. 1998;11:13–9.
3. Kulandai Raja Balan AM, Vasanthi M, Prabu R, Paulraj A, Ramachandramoorthy T. Complexes of Ni(II), Cu(II) and Zn(II) benzoates with nicotinanilide. Int J Modern Chem. 2013;4:66–78.
4. Russell D, Russell AD. Treatment of ringworm: old remedy vs. new. J Infect. 1992;24:333–9.
5. Dendrinou-Samara C, Tsotsou G, Ekateriniadou LV, Kortsaris AH, Raptopoulou CP, Terzis A, Kyriakidis DA, Kessissoglou DP. Anti-inflammatory drugs interacting with Zn(II), Cd(II) and Pt(II) metal ions. J Inorg Biochem. 1998;71:171–9.
6. Sorenson JRJ, Kishore V, Pezeshk A, Oberley LW, Leuthauser SWC, Oberley TD. Copper complexes: a physiological approach to the treatment of inflammatory diseases. Inorg Chim Acta. 1984;91:285–94.
7. Diamantis W, Kohlhepp WC, Haertlein B, Melton J, Sofia RD. Meseclazone, 5-chlorosalicylic acid and acetylsalicylic acid. Comparsion of their effects on in vitro and ex vivo platet aggregation. Thromb Haemost. 1978;40:24–36.
8. Zeleňák V, Győryová K, Mlynarčík D. Antibacterial and antifungal activity of zinc(II) carboxylates with/without N-donor organic ligands. Metal Based Drugs. 2002;8:269–74.
9. Barnes PJ, Drazen JM, Rennard SI, Thomson NC. Asthma and COPD: basic mechanisms and clinical management. 2nd ed. London: Elsevier; 2009. p. 627.
10. Klingsberg E. The chemistry of heterocyclic compounds—pyridine and its derivatives. New York: Wiley; 1962.
11. Kay Brune MD. The early history of non-opionid analgesics. Acute Pain. 1987;1:33–40.
12. Tarushki A, Psomas G, Raptopolou CP, Kessissoglou DP. Zinc complexes of the antibacterial drug oxolinic acid. Structure and DNA-binding properties. J Inorg Biochem. 2009;103:898–905.
13. Klug HP, Alexander LE, Sumner GG. The crystal structure of zinc salicylate dihydrate. Acta Crystallogr. 1958;11:41–6.
14. Brownless NJ, Edwards DA, Mahon MF. Some complexes derived from zinc salicylate or 3,5-di-tert-butylsalicylate. Inorg Chim Acta. 1999;287:89–94.
15. Lemoine P, Viossat B, Dung HD, Tomas A, Morgant G, Greenaway FT, Sorenson JRJ. Synthesis, crystal structures, and anti-convulsant activities of ternary $[Zn^{II}(3,5\text{-diisopropylsalicylate})_2]$, $[Zn^{II}(salicylate)_2]$ and $[Zn^{II}(aspirinate)_2]$ complexes. J Inorg Biochem. 2004;98:1734–49.
16. Sokolík J, Tumová I, Blahová M, Švajnelová O, Švec P. Anti-inflammatory activity of copper(II) and zinc(II) 3,6-dimethylsalicylates and their equimolar mixture. Acta Facultatis Pharm Universitatis Comenianae. 2006;53:224–8.

17. Olczak-Kobza M, Czylkowski R, Karolak-Wojciechowska J. Zinc(II)di(o-hydroxybenzoate) complexes with imidazole and its derivatives. J Therm Anal Calorim. 2003;74:895–904.
18. Olczak-Kobza M, Mrozek A. Zinc(II) and cadmium(II) complexes with o-hydroxybenzoic acid or o-aminobenzoic acid and 2-methylimidazole. J Therm Anal Calorim. 2009;96:553–60.
19. Chomič J, Győryová K, Szunyogová E, Kovářová J. Thermal study of Zinc(II) salicylate complex compounds with bioactive ligands. J Therm Anal Calorim. 2004;76:33–41.
20. Bujdošová Z, Győryová K, Kovářová J, Hudecová D, Halás L. Synthesis, biological and physicochemical properties of Zinc(II) salicylate and 5-chlorosalicylate complexes with theophylline and urea. J Therm Anal Calorim. 2009;98:151–9.
21. Bujdošová Z, Győryová K, Mudroňová D, Hudecová D, Kovářová J. Thermoanalytical investigation and biological properties of zinc(II) 4-chloro- and 5-chlorosalicylates with N-donor ligands. J Therm Anal Calorim. 2012;110:167–76.
22. Bujdošová Z, Győryová K, Hudecová D, Kovářová J, Halás L. Preparation, spectral, thermal, and biological properties of zinc(II) 4-chloro- and 5-chlorosalicylate complexes with methyl-3-pyridylcarbamate and phenazone. Chem Papers. 2010;64:584–91.
23. Köse DA, Necefoğlu H. Synthesis and characterization of bis(nicotinamide) m-hydroxybenzoate complex of Co((II), Ni(II), Cu(II) and Zn(II). J Therm Anal Calorim. 2008;93:509–14.
24. Köse DA, Necefoğlu H, Şahin O, Büyükgüngör O. Synthesis, structural, spectroscopic characterization, and structural comparison of 3-hydroxybenzoate and nicotinamide/*N*,*N*-diethylnicotinamide mixed ligand complex with zinc (II). J Therm Anal Calorim. 2012;110:1233–41.
25. Zaman IG, Debas NC, Necefoğlu H, Hökelek T. trans-Tetraaquabis(isonicotinamide-κN^1) bis(3-hydroxybenzoate) tetrahydrate. Acta Cryst E. 2013;69:m198–9.
26. Icbudak H, Heren Z, Köse DA, Necefoğlu H. bis(nicotinamide) and bis(*N*,*N*-diethylnicotinamide) p-hydroxybenzoate complex of Ni(II), Cu(II) and Zn(II) Spectrothermal studies. J Therm Anal Calorim. 2004;76:837–51.
27. Tyrakowska B, Soffers AEMF, Szymusiak H, Boeren S, Boersma MG, Lemanska K, Vervoort J, Rietjens IMCM. TEAC antioxidant activity of 4-hydroxybenzoates. Free Rad Biol Med. 1999;27:1427–36.
28. Jantová S, Hudecová D, Stankovský Š, Špirková K, Ružeková Ľ. Antibacterial effect of substituted 4-quinazolylhydrazines and their arylhydrazones determined by a modified microdilution method. Folia Microbiol. 1995;40:611–4.
29. Betina V, Mičeková D. Antimicrobial properties of fungal macrolide antibiotics. Z Allg Mikrobiol. 1972;5:355–64.
30. Hudecová D, Jantová S, Melník M, Uher M. New azidometalkojates and their biological activity. Folia Microbiol. 1996;40:473–6.
31. Dudová B, Hudecová D, Pokorný R, Mičková M, Palicová M, Segľa P, Melník M. Copper complexes with bioactive ligands. Part II—antifungal activity. Folia Microbiol. 2002;47:225–9.
32. Graselli JP, Ritchey WM. Atlas of spectral data and physical constants for organic compounds. Ohio: CRC Press; 1975.
33. Nakamoto K. Infrared and raman spectra of inorganic and coordination compounds. New York: Wiley; 1997.
34. Lewandowski W, Kalinowska M, Lewandowska H. The ifluence of metals on the eletronic system of biologically important ligands. Spectroscopic studies of benzoates, salicylates, nicotinates and isoorotates. Review. J Inorg Biochem. 2005;99:1407–23.
35. Findoráková L, Győryová K, Hudecová D, Mudroňová D, Kovářová J, Homzová K, Nour El-Dien FA. Thermal decomposition study and biological characterization of zinc(II) 2-chlorobenzoate complexes with bioactive ligands. J Therm Anal Calorim. 2013;111:1171–781.
36. Zeleňák V, Vargová Z, Győryová K. Correlation of infrared spectra of zinc(II) carboxylates with their structures. Spectrochim Acta. 2007;66:262–72.
37. Smith RM. Understanding mass spectra: a basic approach. 2nd ed. New Jersey: Wiley; 2004.
38. McMurdie H, Morris M, Evans E, Paretzkin B, Wong-Ng W, Ettlinger L, Hubbard C. JCPDS—International Centre for Diffraction Data Task Group on cell parameter refinement. Powder Diffr. 1986;1:66–76.
39. Krajníková A, Győryová K, Hudecová D, Kovářová J. Thermal decomposition and antimicrobial activity of zinc(II) 2-bromobenzoates with organic ligands. J Therm Anal Calorim. 2011;105:451–60.